1 **A unified framework to quantify demographic buffering in natural populations**
2 A manuscript in preparation for submission to ECOLOGY LETTERS
3 Type of article: METHOD
4
5 Gabriel Silva Santos [1,2*], Samuel J L Gascoigne[3*], André Tavares Corrêa Dias[4], Maja Kajin
6 [3,5**♦], Roberto Salguero-Gómez[3♦]
7
8 1 National Institute of the Atlantic Forest (INMA), 29650-000, Santa Teresa, Espírito Santo,
9 Brazil. ssantos.gabriel@gmail.com
10 2 Department of Ecology, Graduate Program in Ecology and Evolution, Rio de Janeiro
11 State University, 524 São Francisco Xavier Street, 20550-900, Maracanã, Rio de Janeiro,
12 Brazil
13 3 Department of Biology, University of Oxford, South Parks Road, OX1 3RB, Oxford, UK.
14 samuel.gascoigne@pmb.ox.ac.uk, rob.salguero@biology.ox.ac.uk,
15 maja.kajin@biology.ox.ac.uk
16 4 Department of Ecology, Institute of Biology, Universidade Federal do Rio de Janeiro,
17 Avenida Carlos Chagas Filho 373, 21941-590 Rio de Janeiro, RJ, Brazil. atcdias@gmail.com
18 5 Department of Biology, Biotechnical Faculty, University of Ljubljana, Večna pot 111, 1000
19 Ljubljana, Slovenia
20
21 *Shared first authorship
22 **Corresponding author
23 ♦Shared senior authorship
24
34
35 RUNNING TITLE: Demographic buffering framework (32/45 characters)
36
37 KEYWORDS: COMADRE Animal Matrix Database, elasticity, life-history evolution,
38 natural selection, second-order derivative, sensitivity, stochasticity, variance.
39
40 NUMBER OF WORDS: Abstract – 143/150 words, main text (excluding abstract,
41 acknowledgements, references, table, and figure legends) – 5713/5000 words
42
43 NUMBER OF REFERENCES: 57
44
45 NUMBER OF TABLES: 1 (in Supplementary Material)
46
47 NUMBER OF FIGURES: 3
48
49

Abstract (143/150 words)

The Demographic Buffering Hypothesis (DBH) predicts that natural selection reduces the temporal fluctuations in demographic processes (such as survival, development, and reproduction), due to their negative impacts on population dynamics. However, a comprehensive approach that allows for the examination of demographic buffering patterns across multiple species is still lacking. Here, we propose a three-step framework aimed at quantifying demographic buffering. Firstly, we categorize species along a continuum of variance based on the sums of stochastic elasticities. Secondly, we examine the linear selection gradients, followed by the examination of nonlinear selection gradients as the third step. With these three steps, our framework overcomes existing limitations of conventional approaches to quantify demographic buffering, allows for multi-species comparisons, and offers insight into the evolutionary forces that shape demographic buffering. We apply this framework to mammal species and discuss both the advantages and potential of our framework.

Environmental stochasticity plays a pivotal role in shaping organisms' life histories (Bonsall & Klug 2011). Nonetheless, how organisms will cope with the increasing variation in environmental conditions expected under climate change (Boyce *et al.* 2006; Morris *et al.* 2008) is one of the most intriguing questions of ecology and evolution (Sutherland *et al.* 2013). Evolutionary demography offers a wide array of explanations for the evolutionary processes that shape the diversity of demographic responses to environmental stochasticity (Charlesworth 1994; Healy *et al.* 2019; Hilde *et al.* 2020; Pfister 1998; Tuljapurkar *et al.* 2009). The Demographic Buffering Hypothesis (*DBH*, hereafter) (Morris & Doak 2004; Pélabon *et al.* 2020) is based on the fact that long-term stochastic population growth rate can be expressed in terms of the geometric mean of the annual population growth rates (Tuljapurkar 1982). As the geometric mean of λ increases, so does the long-term stochastic population growth rate (λ_s, hereafter). However, increases in variance of λ decrease λ_s (Morris & Doak 2004; Tuljapurkar 1982), and thus population persistence. This theoretical context sets the stage for the DBH. The DBH predicts that life histories are under selection pressure to minimise the negative impacts of environmental variation by constraining the temporal variance of those demographic processes (*e.g.*, survival, development, reproduction) to which population growth rate (*i.e.*, fitness) is most sensitive to (Gaillard & Yoccoz 2003; Pfister 1998). The demographic pattern operating the DBH, *i.e.,* demographic buffering, describes the selection-driven constraint on the temporal variance of the most impacting demographic processes for the population growth rate (Hilde *et al.* 2020; Morris & Doak 2004; Pfister 1998). Here, we focus on the latter - on the emerging pattern of demographic buffering in different animal life histories – rather than on the DBH itself.

      A unified approach to unambiguously quantify demographic buffering is still missing. Indeed, identifying demographic buffering remains challenging (Doak *et al.* 2005; Morris & Doak 2004) for at least three reasons. First is the different interpretation of results from

92 correlational analyses (*e.g.*, as in Pfister, 1998). Some authors have used the correlation

93 coefficient as an index to order species' life histories in a continuum ranging from buffered

94 (Spearman's correlation $\rho = <0$ between the sensitivity of λ to demographic processes and

95 their temporal variance) to labile ($\rho = >0$), regardless of the fit of the linear regression to

96 more or less scattered data (McDonald *et al.* 2017). In contrast, other researchers interpret the

97 absence of statistical support for demographic buffering as an alternative strategy where

98 variance in demographic process(es) is favoured to track environmental conditions (the so-

99 called Demographic Lability Hypothesis, *DLH* (*e.g.,*Koons et al. 2009; Reed & Slade 2012;

100 Jäkäläniemi et al. 2013; Hilde et al. 2020). However, the increased temporal variance is a

101 necessary but not sufficient condition to constitute demographic lability – the increased

102 temporal variance needs to lead to (often high) change in the demographic process mean

103 value (Le Coeur *et al.* 2022).

104   The second obstacle to obtain generalisation across species' populations regarding

105 demographic buffering is the hierarchical level at which this phenomenon is <u>typically</u>

106 examined. Some studies base their investigations of demographic buffering on a

107 characteristic drawn from *the entire population model* (*between-populations level*, hereafter)

108 (McDonald *et al.* 2017; Reed & Slade 2012). At the between-populations level, a life history

109 is referred to as demographically buffered if the most important demographic process(es)

110 has(ve) low temporal variance (Le Coeur *et al.* 2022; Hilde *et al.* 2020; Morris & Doak 2004;

111 Pfister 1998). However, to understand how, why, and where demographic buffering occurs –

112 or not– and how buffering patterns might be modified in response to the environment, it is

113 essential to also consider the characteristics of the separate *components of population model*

114 (*within-populations level*, hereafter). Within a population, a given demographic process can

115 be buffered against while another can be labile to the environment (Barraquand & Yoccoz

116 2013; Jongejans *et al.* 2010; Koons *et al.* 2009). Thus far, studies have focused on either one

117   of the hierarchical levels, however, for a mechanistic understanding of how environmental

118   stochasticity shapes life histories, both between- and within-population levels need to be

119   addressed at the same time.

120   The third reason limiting a holistic understanding of demographic strategies in

121   stochastic environments are the challenges inherent to examining their underlying

122   mechanisms. Evidence for demographic buffering exists across some long-lived organisms

123   with complex life cycles, (Doak *et al.* 2005; Gaillard & Yoccoz 2003; McDonald *et al.* 2017;

124   Pfister 1998; Rotella *et al.* 2012), but also in short-lived species (Ferreira *et al.* 2013; Pfister

125   1998; Reed & Slade 2012). Importantly, these patterns of variation do not inform entirely on

126   how the life histories were shaped by natural selection. The beforementioned patterns of

127   variation are represented by *first-order* effects that perturbations in demographic processes

128   cause on the population growth rate (*i.e.,* elasticities). A first order effect informs us

129   regarding the population growth rate's sensitivity to *variation in demographic processes*.

130   While a second-order effect of perturbations in demographic processes reveals the population

131   growth rate's sensitivity to *autocorrelation* (Tuljapurkar 1990). Given so, integrating both,

132   first and second-order effects of perturbations in demographic processes on the population

133   growth rate, allows us to understand the behaviour of the fitness function at the vicinity of the

134   local maxima and/or minima.

135   When the relationship between fitness and a demographic process is linear, the

136   second-order derivatives of population growth rate with respect to demographic processes

137   equal zero. In such cases, natural selection acts on the mean value of a demographic process

138   (Shyu & Caswell 2014). However, nonzero second derivatives indicate a nonlinear

139   relationship between fitness and a demographic process (either concave if <0, or convex if

140   >0) and thus provide additional and often overlooked characteristics of selection acting on

demographic processes – not only their mean values, but also their variances and covariances

(Brodie *et al.* 1995; Carslake *et al.* 2008; Shyu & Caswell 2014).

The sign (*i.e.*, >0, =0, <0) of the self-second derivative of λ with respect to

demographic processes determines the type of (non)linear selection acting on a demographic

process. For instance, a negative self-second derivative for a given demographic process

describes a concave form of selection, commonly referred to as the ∩-shaped selection

(Caswell 1996, 2001; Shyu & Caswell 2014). This form of selection reduces the temporal

variance in said demographic process, thereby providing evidence of demographic buffering.

Conversely, a demographic process yielding a positive self-second derivative identifies a

convex, or ∪-shaped selection (Caswell 1996, 2001; Shyu & Caswell 2014). Such a selection

mechanism acts upon demographic processes amplifying their temporal variance, thus

potentially evidencing demographic lability (Le Coeur et al. 2022; Koons et al. 2009). The

evidence of lability is only potential, because to constitute demographic lability, the increased

variance needs to shift the mean value of a demographic process. The shift in the mean value

of a demographic process needs to overweight the negative effect of variance on the

population growth rate (Le Coeur *et al.* 2022).

The rich variation in demographic strategies across the Tree of Life is a result of

evolutionary processes that have shaped variance in demographic processes through time. In

this context, setting demographic buffering into the adaptive landscape context of linear and

nonlinear selection enables us to identify and quantify the evolutionary processes that

generate said demographic patterns. In this way, one will better understand how increased

variability of environmental conditions might act on the existing –and shape novel–

demographic strategies. However, we still lack a unified approach to constitute the signatures

of demographic buffering.

165   Here, we present a framework that quantifies demographic buffering. Our framework

166   provides a rich insight into the patterns of temporal variance in demographic processes

167   affected by environmental stochasticity. This framework involves categorizing species or

168   populations along a variance continuum based on the extent to which key demographic

169   processes are buffered by natural selection, thereby limiting their temporal variability. The

170   framework consists of four steps with a mix of well-known methods applied to stage-

171   structured demographic information (*e.g.,* matrix population models [Caswell 2001]; integral

172   projection models [Easterling et al. 2000]). First, we position species or populations on the

173   aforementioned continuum to assess the cumulative effect of the variance in their key

174   demographic processes on population growth rate at the between-populations level (see

175   below). Second, we investigate the presence of linear selection forces operating within the

176   life cycle of each species or population at the within-populations level (below). Third, we

177   explore the impact of non-linear selection forces acting within the life cycle of each species

178   or population, also at the within-populations level. The combination of these three steps

179   provides quantitative evidence for the occurrence of demographic buffering. Step four

180   suggests the further necessary analyses to identify demographic lability.

181   To demonstrate the applicability of our framework, we apply it to 40 populations of

182   34 mammal species sourced from the COMADRE database (Salguero-Gómez *et al.* 2016).

183   We showcase how the framework can provide valuable insights into the patterns of

184   demographic buffering across species. The framework offers novel, detailed insights into the

185   selection pressures that act *within* species' life cycles, thus allowing for a thorough

186   understanding of the evolutionary selection forces that shape the patterns of demographic

187   buffering across species. Beyond providing a quantitative, systematic toolset to quantify

188   buffering through three steps, we have also offer an alternative fourth step that briefly

189   outlines how to evidence lability.

190

A unified framework to assess evidence of demographic buffering

The evidence for demographic buffering has been mainly assessed using Matrix
Population Models (MPM; Pfister 1998; Rotella et al. 2012)). However, Integral Projection
Models (IPM; Rodríguez-Caro et al. 2020; Wang et al. 2023) can be equally applied for
identifying the demographic buffering signatures. Both MPMs and IPMs are stage-structured,
discrete-time demographic models (Caswell 2001; Ellner *et al.* 2016). For simplicity, here we
focus on MPMs, but note that the same approaches are as equally applicable to IPMs (Doak
et al. 2021; Griffith 2017). Throughout this manuscript, we refer to demographic processes as
both matrix entries a_{ij} (*i.e.,* upper-level parameters) and the vital rates that underline the
matrix elements (*i.e.,* lower-level parameters), and note that their conversion is
straightforward and described elsewhere (Franco & Silvertown 2004). The framework
operates on three steps.

The first step of our framework involves acquiring the relative impact of variation in
demographic processes on the stochastic growth rate, λ_s, the so-called stochastic elasticities,
E_{ij}^S (Haridas & Tuljapurkar 2005) (Figure 1A). The sum of all stochastic elasticities ($\Sigma E_{a_{ij}}^S$),
can be separated into two components to assess how temporal variance and mean values of
each demographic process impact λ_s. The first component represents the *sum of stochastic*
elasticity of λ_s with respect to the variance $\Sigma E_{a_{ij}}^{S^\sigma}$, and the second represents the *sum of*
stochastic elasticity of λ_s with respect to the mean $\Sigma E_{a_{ij}}^{S^\mu}$, where $\Sigma E_{a_{ij}}^S = \Sigma E_{a_{ij}}^{S^\sigma} + \Sigma E_{a_{ij}}^{S^\mu}$
(Haridas & Tuljapurkar 2005). Thus, the summation $\Sigma E_{a_{ij}}^{S^\sigma}$ quantifies the summed effect to
which the stochastic population growth rate (λ_s) is influenced by changes in the variances of
the demographic processes within the population matrix.

213   A higher sum of stochastic elasticity of λ_s with respect to the variance of demographic

214   processes (*i.e.,* higher absolute value; $|\Sigma E_{a_{ij}}^{S^\sigma}|$) indicates that small changes in the variance of

215   demographic processes would have a substantial impact on λ_s. In other words, the variance of

216   that demographic process is not constrained by selection, indicating absence of demographic

217   buffering. On the other hand, a lower (absolute) stochastic elasticity of λ_s with respect to the

218   variance of a given demographic process suggests that λ_s is less sensitive to such

219   perturbations, or, that variance of such demographic process is being constrained by natural

220   selection, thus pointing to demographic buffering (Haridas & Tuljapurkar 2005; Tuljapurkar

221   *et al.* 2003) (Fig. 1A).

222   The first step of the framework thus features the between-populations level and places

223   species or populations alongside a continuum. Species exhibiting unconstrained variance in

224   demographic processes (*i.e.,* possibly not buffered, Fig. 1A, blue dots) are positioned on the

225   left-hand side of the continuum. In contrast, species with constrained variance in

226   demographic processes (*i.e.,* possibly buffered, Fig. 1A, yellow dots) are positioned on the

227   right-hand side of the continuum. However, the left-hand side of the continuum does not

228   necessarily imply evidence of demographic lability. This is so because demographic lability

229   is defined as an increase in the *mean value* of a demographic process in response to improved

230   environmental conditions (Le Coeur *et al.* 2022). By examining $\Sigma E_{a_{ij}}^{S^\sigma}$, we can visualize an

231   increase or decrease of the contribution that *variance* of demographic processes has on the

232   long-term population growth rate, while the mean value of a demographic process does not

233   change.

234   Step 1 of our framework examines the impacts that environmental variation has on the

235   long-term population growth rate, λ_s (Tuljapurkar *et al.* 2003). This means that the resulting

236   variance continuum in this step of the framework is based on how λ_s was affected by

237   variation in the key demographic parameter across all contiguous time periods. However,

238 Haridas & Tuljapurkar (2005) explicitly acknowledge that covariances between demographic

239 processes and serial correlations need to be investigated to diagnose buffering entirely. Our

240 approach does not use covariances neither serial correlation, but rather focuses on the second

241 derivatives of the population growth rate with respect to demographic processes and

242 elucidates how selection is acting on variance (step 3, below).

243   Steps 2 and 3 of the framework are conducted at the within-populations level. Once

244 species or populations are positioned along the variance continuum regarding the summed

245 effect of variation on λ_s, (step 1), one needs to zoom into each life cycle separately, analysing

246 the selection pressures acting on each one of the demographic processes composing the life

247 cycle (*i.e.,* population model). In doing so, one can inspect the selection pressures that have

248 generated the patterns found in step 1. Step 2 (Fig. 1B) requires obtaining the partial

249 derivatives of the deterministic population growth rate, λ_t, relative to all matrix elements of

250 the MPM of interest (*i.e.,* elasticities of λ_t w.r.t each demographic process in the MPM). Step

251 2 therefore informs on the impact that each of the demographic processes has on λ_t

252   Finally, in step 3, one assesses the pattern of nonlinear selection by using the self-

253 second derivatives of λ_t with respect to each demographic process (Fig. 1C). This step reveals

254 the potential nonlinear selection pressures on each of the demographic processes within a life

255 cycle. This step is key to understanding the evolutionary processes (*i.e.,* types of nonlinear

256 selection) that the demographic processes are subjected to. Without understanding the

257 evolutionary processes operating on the demographic processes, the pattern observed in step

258 1 might be artefactual. (e.g., Lawler et al. 2009)

259   Steps 2 and 3 of the framework feature selection pressures that have been averaged

260 over the contiguous time periods. This means that the resulting patterns are based on how λ_t

261 (obtained from averaging all sequential MPMs across the duration of the study) would be

262 affected if a demographic process were perturbed. Therefore, steps 2 and 3 are based on a

263   different information than step 1 and can thus complete our understanding of the role of

264   selection pressures on shaping demographic patterns across multiple species.

265   Another important asset of step 3 above includes the notion that the relative

266   importance (elasticity) of demographic processes themselves changes with changing

267   environment (Stearns 1992). In other words, the extent to which λ_t is sensitive to

268   perturbations in a specific demographic process is *dynamic* (Kroon *et al.* 2000). Thus, the

269   self-second derivatives generate information on how the sensitivity (or elasticity) of λ_t might

270   change. If the sensitivity (or elasticity) of λ_t can change, then it is important to know which

271   demographic processes are most prone to trigger such a change. In the example of a

272   hypothetical wolf species (Fig. 1), this means that if the reproduction of the third age-class

273   individuals (matrix element $a_{1,3}$) decreased, the sensitivity of λ_t to $a_{1,3}$ would increase (square

274   with the largest black dot, Fig. 1C). Consequently, with increased environmental variability,

275   the key demographic process might change from remaining in the fourth age class (matrix

276   element $a_{4,4}$, Fig. 1B) to reproduction of the third age-class (matrix element $a_{1,3}$, Fig. 1C).

277   Combining the three steps of our framework allows for a quantitative identification of

278   buffering. Steps 2 and 3 offer key insights as to *why* a given species or population is placed

279   on either the buffered or the non-buffered end of the variance continuum. A clear and

280   unequivocal evidence for support towards buffering consists of: (1) a species or population

281   being positioned near the 0 end of the continuum (the right-hand side) in step 1; (2) this

282   species' or populations' life cycle having one or more demographic processes with highest

283   elasticity values in step 2; and (3) the same demographic process displaying the highest

284   elasticity in step 2 with negative self-second derivative values in step 3. In this sense, Figure

285   1B shows that, for the chosen population of a hypothetical wolf species, the most important

286   demographic process is remaining in the fourth stage (MPM element $a_{4,4}$), as this

287   demographic process results in highest elasticity value (Fig. 1B yellow square). However,

288   Fig. 1C reveals that $a_{4,4}$ is under little selection pressure for variance reduction. Thus, there is

289   no clear evidence of buffering from the third step of the framework (*i.e.,* no concave selection

290   forces).This way, the lack of concave selection forces on the key demographic process within

291   wolf's life cycle explains why this species is placed on the left-hand side of the variance

292   continuum (Fig. 1A).

293   Species placed on the non-buffered end of the continuum is a necessary but not

294   sufficient condition for evidence demographic lability. It is key highlighting here that

295   demographic buffering and lability do not represent two extremes of the same continuum.

296   The variance continuum allocates the species or populations from strongly buffered to non-

297   buffered, but to test the for lability, a further step is needed.

298   Although not our primary goal here, we briefly introduce said step 4. To establish

299   compelling evidence of lability, it is essential to fulfil several further criteria. First, sufficient

300   data across various environments (over time or space) are required to construct reaction

301   norms that depict how a demographic process responds to environmental changes (Morris et

302   al., 2008; Koons et al., 2009), which can be challenging in terms of sufficient and high-

303   quality demographic and environmental data. Second, non-linear relationships between

304   demographic processes and the environment must be established based on the demographic

305   process-environment reaction norms. Lastly, demographic processes where an increase in the

306   mean value has a stronger positive impact on population growth rate than the detrimental

307   effect of increased variance needs to be identified. The latter condition is only met when the

308   demographic process-environment reaction norm takes a convex shape (resembling a "∪"

309   shape), as described by Koons et al. (2009) and Morris et al. (2008). However, a study by

310   Barraquand and Yoccoz (2013) reported diverging results in this regard. Importantly, we note

311   that more likely than previously thought (*e.g.,* Pfister 1998), species do not exist as purely

312   buffering or labile, but that within populations, some vital rates may be buffered, other labile,

313 and others insensitive to the environment (*e.g.*, (Doak *et al.* 2005). Deciphering generality in

314 this likely complex pattern should attract much research attention going forward, in our

315 opinion.

316

317 **Demographic buffering in mammals: a case study using the unified framework**

318 We demonstrate the performance of our framework using 44 MPMs from 34 mammal

319 species. Mammals are of special interest here for two reasons: (1) mammalian life histories

320 have been well studied (Bielby *et al.* 2007; Gillespie 1977; Jones 2011; Stearns 1983); and

321 (2) some of their populations have already been assessed in terms of buffering, particularly

322 for primates (Campos *et al.* 2017; Morris *et al.* 2008, 2011; Reed & Slade 2012; Rotella *et al.*

323 2012). Together, the well-studied life histories and previous information about the occurrence

324 of buffering in mammals provide the necessary information to make accurate predictions and

325 validate the performance of the proposed framework.

326 We used Matrix Population Models from 40 out of 139 studies with mammals

327 available in the COMADRE database v.3.0.0 (Salguero-Gómez *et al.* 2016). These 40

328 populations encompass 34 species from eight taxonomic orders. We included these MPMs in

329 our analyses because they provide values of demographic processes (a_{ij}) for three or more

330 contiguous time periods, thus allowing us to obtain the stochastic elasticity of each a_{ij}.

331 Although we are aware that not all possible temporal variation in demographic processes may

332 have been expressed within this period, we assumed three or more transitions are enough to

333 provide sufficient variation for population comparison. At least three contiguous time periods

334 - a common selection criteria in comparative studies of stochastic demography (Compagnoni

335 *et al.* 2023) - also allowed to test and showcase our framework. Fortunately, several long-

336 lived species, characterized by low variation in their demographic processes, were studied for

337 a long time (*e.g.,* some primates in our dataset have been studied for over 20 years – Morris

338 *et al.* 2011). We removed the populations where either only survival or only reproduction

rates were reported, because of the impossibility to calculate the stochastic growth rate. A

detailed description of the analysed data and their original sources are available in

supplementary material (Supplementary Material, Table S1).

Homo sapiens was included in our analyses because it is the only mammalian species

in which second-order derivatives have been applied (Caswell 1996). Therefore, Homo

sapiens provides an ideal basis for comparisons among species. The data for Homo sapiens

were gathered from 26 modern populations located in various cities, allowing us to construct

a spatiotemporal variance. It is important to note that in this case, we are not working with

true temporal variance but rather a variance that encompasses both spatial and temporal

aspects.

For steps 2 and 3 of our framework, we utilized a subset of 16 populations (including

Homo sapiens) whose population projection matrices (MPMs) were organized by age. We

specifically selected these populations because their life cycles can be summarized by two

main demographic processes: survival and contribution to recruitment of new individuals.

The contribution to recruitment can be interpreted as either the mean reproductive output for

each age class or an approximation thereof, depending on how the matrices are structured

(Ebert 1999). One advantage of using such matrices is that they encompass only two types of

demographic processes, namely survival and recruitment, eliminating the need to account for

multiple transitions between different life stages.

To perform the step 1 of our framework and obtain the $\Sigma E_{a_{ij}}^{S^\sigma}$ (and $\Sigma E_{a_{ij}}^{S^\mu}$), we followed

Tuljapurkar $et\ al.$ (2003) and Haridas & Tuljapurkar (2005). To perform step 2 of our

framework, we calculated the deterministic elasticities of each demographic process extracted

using the $popbio$ package. All analyses were performed using R version 3.5.1 (R Core team,

2018). Finally, to perform the step 3 of our framework the self-second derivatives were

363   adapted from *demogR* (Jones 2007) following (Caswell 1996) and applied for the mean

364   MPM.

365   *Results*

366   We ranked 40 populations from the 34 identified mammal species according to the

367   cumulative impact of variation in demographic processes on λ_s using the step 1 of our

368   framework (Fig. 2). Additional information (including standard deviations of the elasticity

369   estimates and number of matrices available) is provided in the supplementary material (Table

370   S1). Most of the analysed orders were placed on the low-variance end of the variance

371   continuum (Fig. 2). The smallest contributions of variation in demographic processes (*i.e.,*

372   maximum value of $\Sigma E_{a_{ij}}^{S^{\sigma}}$, note that $\Sigma E_{a_{ij}}^{S^{\sigma}}$ ranges from 0 to -1), suggesting more buffered

373   populations, were assigned to Primates: northern muriqui (*Brachyteles hyphoxantus*, $\Sigma E_{a_{ij}}^{S^{\sigma}}$ = -

374     $0.09 \times 10^{-4} \pm 0.12 \times 10^{-4}$) (mean ± standard deviation) (Fig. 2 silhouette a), mountain gorilla

375   (*Gorilla beringhei*, $\Sigma E_{a_{ij}}^{S^{\sigma}}$ = $-0.24 \times 10^{-4} \pm 0.08 \times 10^{-4}$) (Fig. 2 silhouette b), followed by the

376   blue monkey (*Cercopithecus mitis*, $\Sigma E_{a_{ij}}^{S^{\sigma}}$ = $-0.63 \times 10^{-4} \pm 0.06 \times 10^{-4}$) (Fig. 2 silhouette c).

377   The first non-primate species placed near the low-variance end of the continuum was the

378   Columbian ground squirrel (*Urocitellus columbianus*, Rodentia, $\Sigma E_{a_{ij}}^{S^{\sigma}}$ = -0.003 ± 0.002) (Fig.

379   2 silhouette d). The species with the highest contribution of variation in demographic

380   processes placed at the high-variance end of the continuum was the stoat (*Mustela erminea*,

381   Carnivora, $\Sigma E_{a_{ij}}^{S^{\sigma}}$ = -0.35 ± 0.02) (Fig. 2 silhouette e). All the 14 primate populations

382   displayed potential evidence of buffering, occupying the right-hand side of the variance

383   continuum, with the exception of the Patas monkey (*Erythrocebus patas*, Primates, $\Sigma E_{a_{ij}}^{S^{\sigma}}$ = -

384   0.05 ± 0.03) (Fig. 2 silhouette f). The snowshoe hare (*Lepus americanus*, Lagomorpha, $\Sigma E_{a_{ij}}^{S^{\sigma}}$

385   = -0.29 ± 0.16) (Fig. 2 silhouette g) and the Bush rat (*Rattus fuscipes*, Rodentia, $\Sigma E_{a_{ij}}^{S^\sigma}$ = -0.25

386   ± 0.03) (Fig. 2 silhouette h) appear on the high-variance end of the continuum.

387   As predicted for the steps 2 and 3, we could not observe a clear pattern in support of

388   buffering. This finding means that the demographic processes with the highest elasticity

389   values failed to display strongly negative self-second derivatives (Fig. 3). Particularly for

390   majority of primates - with the lack or minor temporal variation in demographic processes -

391   demographic processes with high elasticities had positive values for the self-second

392   derivatives (indicated by yellow squares with white dots in Fig. 3). Examples of primate

393   species exhibiting high elasticities and positive values for the self-second derivatives and

394   include northern muriqui (*Brachyteles hypoxanthus*), mountain gorilla (*Gorilla beringei*),

395   white-faced capuchin monkey (*Cebus capucinus*), rhesus monkey (*Macaca mulatta*), blue

396   monkey (*Cercopithecus mitis*), Verreaux's sifaka (*Propithecus verreauxi*) and olive baboon

397   (*Papio cynocephalus*) (Fig. 3). This implies that the key demographic processes influencing

398   λ_t are not subject to selective pressure for reducing their temporal variability. However, even

399   though the primates were positioned closer to the low-variance end of the continuum in step

400   1, the evidence from steps 2 and 3 does not support the occurrence of buffering in the most

401   influential demographic processes.

402   The killer whale showed similar controversy between step 1 and steps 2-3 results as

403   most primates. In step 1, the killer whale was positioned at the buffered end of the variance

404   continuum (*Orcinus orca*, Cetacea, $\Sigma E_{a_{ij}}^{S^\sigma}$ = -0.70 × 10^{-4} ± 1.04 × 10^{-5}) (Fig. 2 silhouette not

405   shown). However, steps 2 and 3 show that the three demographic processes in killer whale

406   life cycle with highest elasticity values (matrix elements $a_{2,2}$, $a_{3,3}$ and $a_{4,4}$) are not under

407   selection pressures for reducing their temporal variance, but the opposite (depicted by yellow

408   and green squares with white dots, Fig. 3).

16

409   The only primate species exhibiting evidence of buffering in steps 2 and 3 was

410 human. In human, demographic parameters representing survival from first to second age

411 class (matrix element $a_{2,1}$) displayed high elasticities and negative self-second derivatives

412 (depicted as yellow squares with black dots in Fig. 3). Evidence supporting buffering was

413 also found in the Columbian ground squirrel (*Urocitellus columbianus*), where, similar to

414 humans, survival from the first to the second age class (matrix element $a_{2,1}$) showed

415 indications of selection acting to reduce $a_{2,1}$variance. Accordingly, the Columbian ground

416 squirrel was positioned close to the buffered end of the variance continuum in step 1. Hence,

417 the Columbian ground squirrel was the sole species with consistent evidence of buffering

418 across all three steps of the framework.

419   The Soay sheep (*Ovis aries*) was the species furthest from the buffered end of the

420 variance continuum that enabled to perform steps 2 and 3. For the Soay sheep, remaining in

421 the third age class (matrix element $a_{3,3}$) has the major influence on λ_t and is under selection

422 pressure to have its variance increased. The latter characteristics reveal potential conditions

423 for lability even though the species is placed closer to the buffered end of the variance

424 continuum.

425   Steps 2 and 3 illustrate the importance of examining buffering evidence on the within-

426 populations level. These two steps of the framework identify the simultaneous acting of

427 concave and convex selection on different demographic processes within a single life cycle.

428 In polar bear (*Ursus maritimus*), the key demographic process (matrix element $a_{4,4}$) is under

429 convex selection, as depicted by a yellow square with a white dot in Fig. 3. However, the

430 demographic process with the second highest elasticity value (matrix element $a_{5,4}$) is under

431 strong concave selection (depicted by a light green square with a black dot in Fig. 3).

432   By adding step 3 to the framework, another important information was accessed. The

433   high absolute values of self-second derivatives (large dots, either black or white, Fig. 3)

434   indicate where the sensitivity of λ_t to demographic parameters is itself prone to environmental

435   changes. For instance, if the value of $a_{5,4}$ for polar bear increased, the sensitivity of λ_t to $a_{5,4}$

436   would decrease because the self-second derivative of $a_{5,4}$ is highly negative (depicted by the

437   largest black dot in polar bear MPM). Vice versa holds for the $a_{4,4}$ demographic process,

438   where an increase in the value of $a_{4,4}$ would increase λ_t's sensitivity to $a_{4,4}$, because the self-

439   second derivative of $a_{5,4}$ is highly positive (depicted by the largest white dot in polar bear

440   MPM). Thus, sensitivities (or equally elasticities) of demographic processes with high

441   absolute values for self-second derivatives can easily change..

Discussion

443   In the Anthropocene, identifying and quantifying mechanisms of species responses to

444   stochastic environments holds crucial importance. This importance is particularly tangible in

445   the context of the unprecedented environmental changes and uncertainties that impact the

446   dynamics and persistence of natural populations (Boyce *et al.* 2006). Correlational

447   demographic analysis, whereby the importance of demographic processes and their temporal

448   variability is examined (Pfister 1998), has attempted to identify how species may buffer

449   against the negative effects of environmental stochasticity. However, these widely used

450   approaches have important limitations (see Introduction and Hilde et al. 2020). One

451   significant limitation is the issue of measurement scale concerning demographic processes

452   (Hilde *et al.* 2020; Morris & Doak 2004). Demographic processes, such as birth rates, death

453   rates, immigration, and emigration, operate at various temporal and spatial scales. The choice

454   of scale at which these processes are measured can impact the outcomes of correlational

455   demographic analysis (Bjørkvoll *et al.* 2016). Our novel framework overcomes said

456   limitations by providing a rigorous approach to quantify demographic buffering (Hilde et al.

457   2020; Pfister 1998).

458   Evidencing demographic buffering is not straightforward. Indeed, through the

459   analysis of stochastic population growth rate (λ_s) in our application of the framework to 44

460   populations of 34 species, we identify the highest density of natural populations near the

461   buffered end of the variance continuum (step 1). However, we show that the same species

462   then fail to exhibit signs of concave (∩-shaped) selection on the key demographic parameters

463   when further analyses are performed averaging the variation across the duration of each study

464   (steps 2 and 3). This finding confirms that placing the species near the buffered end of the

465   variance continuum is *necessary* but not *sufficient* to diagnose demographic buffering.

466   Indeed, buffering occurs when concave selection forces act on the key demographic

467   parameter (Caswell 1996, 2001; Shyu & Caswell 2014).

468   Combining the three steps into a unified framework is of outmost importance. In steps

469   2 and 3 of the framework, we find relatively limited overall evidence of buffering in the

470   examination of our 16 (out of 34 in step 1) studied animal species. Step 3 of our framework

471   reveals that the role of natural selection shaping temporal variation in demographic processes

472   is more complex than expected. Indeed, demographic processes within our study populations

473   are often under a mix of convex and concave selection. This mix of selection patterns was

474   already suggested by Doak *et al.* (2005). Here, only two out of 16 mammal species revealed

475   concave selection acting on the key demographic processes (Columbian ground squirrel

476   [*Urocitellus columbianus*], and humans, [*Homo sapiens sapiens*]). These two species were

477   also placed near the buffered end of the variance continuum, therefore meeting all the

478   necessary conditions to diagnose buffering. However, finding 12.5% (two out of 16) species

479   that meet the criteria for demographic buffering is not in concordance with previous studies.

480   Evidence of buffering has been reported across 22 ungulate species (Gaillard & Yoccoz

481 2003). In the one ungulate we examined, the moose (*Alces alces*), we find only partial

482 support for buffering in adult survival, since this species is placed near the buffered end of

483 the variance continuum in step 1 but does not show concave selection pressures on adult

484 survival in step 2/3, as would be necessary to confirm the occurrence of buffering.

485 It is worth noting that a varying number of matrices per species were employed, ranging from

486 1 to 21, with an average of 8.1 matrices per species (as shown in Table S1). Naturally, having

487 a greater number of matrices is preferred in such analyses. Furthermore, while the size of

488 matrices (matrix dimensions) does not directly bias the results of our framework in any way –

489 since steps 2 and 3 are shown for all the demographic processes independent of matrix

490 dimension – potential implications of varying matrix dimensions should be further

491 investigated in the future.

492   Our overall findings reveal varying levels of support for the notion that adult survival

493 in long-lived species tends to be buffered. Indeed, Gaillard *et al.* (1998) found that adult

494 female survival varied considerably less than juvenile survival in large herbivores. This

495 finding was also supported by further studies in ungulates and small rodents (Gaillard &

496 Yoccoz 2003), turtles (Heppell 1998), vertebrates and plants (Pfister 1998), and more

497 recently across nine (out of 73) species of plants (McDonald *et al.* 2017).

498   When placing our study species along a variance continuum (step 1), primates tend to

499 be located on the buffered end. However, most primates displayed convex –instead of the

500 expected concave– selection on adult survival. Similar results, where the key demographic

501 process failed to display constrained temporal variability, have been reported for long-lived

502 seabirds (Doherty *et al.* 2004). One explanation for the unexpected convex selection on adult

503 survival involves trade-offs, as suggested by (Doak *et al.* 2005). When two demographic

504 parameters are negatively correlated, the variance of population growth rate (λ) can be

505 increased or decreased (Compagnoni *et al.* 2016; Evans & Holsinger 2012). The well-

506   established trade-off between survival and fecundity (Roff & Fairbairn 2007; Stearns 1992)

507   might explain the observed deviation of our results. Because variation in primate recruitment

508   is already constrained by physiological limitations (Campos *et al.* 2017), when adult survival

509   and recruitment are engaged in a trade-off, this trade-off might lead to our unexpected result.

510   Correlations among demographic processes (positive and negative) inherently influence the

511   biological limits of variance (Haridas & Tuljapurkar, 2005). This is because the magnitude of

512   variation in a particular demographic process is constrained by (the variation of) other

513   demographic processes that exert an influence on it. Not surprisingly, correlations among

514   demographic processes have been shown to be strongly subjected to ecological factors (Fay

515   *et al.* 2022). Here, future studies may benefit from deeper insights via cross-second

516   derivatives (Caswell 1996, 2001) to investigate correlations among demographic processes.

517   Examining the drivers of demographic buffering has become an important piece of the

518   ecological and evolutionary puzzle of demography. As such, quantifying buffering can help

519   us better predict population responses to environmental variability, climate change, and direct

520   anthropogenic disturbances (Boyce *et al.* 2006; McDonald *et al.* 2017; Pfister 1998; Vázquez

521   *et al.* 2017). By setting demographic buffering into a broader and integrated framework, we

522   hope to enhance comprehension and prediction of the implications of heightened

523   environmental stochasticity on the evolution of life history traits. This understanding is

524   crucial in mitigating the risk of extinction for the most vulnerable species.

525

532

533   **Data availability**

534   The demographic data used in this paper are open-access and available in the COMADRE

535   Animal Matrix Database (https://compadre-db.org/Data/Comadre). A list of the studies and

536   species used here is available in Supplementary Material (Table S1). The data and code

537   supporting the results can be accessed here:

538   https://github.com/SamuelGascoigne/Demographic_buffering_unified_framework.

539

540   **References**

541   Barraquand, F. & Yoccoz, N.G. (2013). When can environmental variability benefit
542   population growth? Counterintuitive effects of nonlinearities in vital rates. *Theor Popul*
543   *Biol*, 89, 1–11.

544   Bielby, J., Mace, G.M., Bininda-Emonds, O.R.P., Cardillo, M., Gittleman, J.L., Jones, K.E.,
545   *et al.* (2007). The Fast-Slow Continuum in Mammalian Life History: An Empirical
546   Reevaluation. *Am Nat*, 169, 748–757.

547   Bjørkvoll, E., Lee, A.M., Grøtan, V., Saether, B.-E., Stien, A., Engen, S., *et al.* (2016).
548   Demographic buffering of life histories? Implications of the choice of measurement
549   scale. *Ecology*, 97, 40–47.

550   Bonsall, M.B. & Klug, H. (2011). The evolution of parental care in stochastic environments.
551   *J Evol Biol*, 24, 645–655.

552   Boyce, M.S., Haridas, C. V., Lee, C.T., Boggs, C.L., Bruna, E.M., Coulson, T., *et al.* (2006).
553   Demography in an increasingly variable world. *Trends Ecol Evol*, 21, 141–148.

554   Brodie, E.I., Moore, A. & Janzen, F. (1995). Visualizing and quantifying natural selection.
555   *Trends Ecol Evol*, 10, 313–318.

556   Campos, F.A., Morris, W.F., Alberts, S.C., Altmann, J., Brockman, D.K., Cords, M., *et al.*
557   (2017). Does climate variability influence the demography of wild primates? Evidence
558   from long-term life-history data in seven species. *Glob Chang Biol*, 23, 4907–4921.

559   Carslake, D., Townley, S. & Hodgson, D.J. (2008). Nonlinearity in eigenvalue-perturbation
560   curves of simulated population projection matrices. *Theor Popul Biol*, 73, 498–505.

561   Caswell, H. (1996). Second Derivatives of Population Growth Rate: Calculation and
562   Applications. *Ecology*, 77, 870–879.

563 Caswell, H. (2001). *Matrix Population Models: Construction, Analysis, and Interpretation*.
564   Sinauer Associates Inc. Publishers, Sunderland, Massachusetts, USA.

565 Charlesworth, B. (1994). *Evolution in age-structured populations*. second edi. Cambridge
566   University Press.

567 Le Coeur, C., Yoccoz, N.G., Salguero-Gómez, R. & Vindenes, Y. (2022). Life history
568   adaptations to fluctuating environments: Combined effects of demographic buffering
569   and lability. *Ecol Lett*, 1–13.

570 Compagnoni, A., Bibian, A.J., Ochocki, B.M., Rogers, H.S., Schultz, E.L., Sneck, M.E., *et*
571   *al.* (2016). The effect of demographic correlations on the stochastic population dynamics
572   of perennial plants. *Ecol Monogr*, 86, 480–494.

573 Compagnoni, A., Evers, S. & Knight, T. (2023). Spatial replication can best advance our
574   understanding of population responses to climate. *bioRxiv*,
575   https://doi.org/10.1101/2022.06.24.497542.

576 Doak, D.F., Morris, W.F., Pfister, C., Kendall, B.E. & Bruna, E.M. (2005). Correctly
577   Estimating How Environmental Stochasticity Influences Fitness and Population Growth.
578   *Am Nat*, 166, E14–E21.

579 Doak, D.F., Waddle, E., Langendorf, R.E., Louthan, A.M., Isabelle Chardon, N., Dibner,
580   R.R., *et al.* (2021). A critical comparison of integral projection and matrix projection
581   models for demographic analysis. *Ecol Monogr*, 91, e01447.

582 Doherty, P.F., Schreiber, E.A., Nichols, J.D., Hines, J.E., Link, W.A., Schenk, G.A., *et al.*
583   (2004). Testing life history predictions in a long-lived seabird: A population matrix
584   approach with improved parameter estimation. *Oikos*, 105, 606–618.

585 Easterling, M.R., Ellner, S.P. & Dixon, P.M. (2000). Size-Specific Sensitivity: Applying a
586   New Structured Population Model. *Ecology*, 81, 694–708.

587 Ellner, S.P., Childs, D.Z. & Rees, M. (2016). *Data-driven Modelling of Structured*
588   *Populations. A practical guide to the Integral Projection Model*. Lecture Notes on
589   Mathematical Modelling in the Life Sciences. Springer International Publishing, Cham.

590 Evans, M.E.K. & Holsinger, K.E. (2012). Estimating covariation between vital rates : A
591   simulation study of connected vs . separate generalized linear mixed models (GLMMs).
592   *Theor Popul Biol*, 82, 299–306.

593 Fay, R., Hamel, S., van de Pol, M., Gaillard, J.M., Yoccoz, N.G., Acker, P., *et al.* (2022).
594   Temporal correlations among demographic parameters are ubiquitous but highly
595   variable across species. *Ecol Lett*, 25, 1640–1654.

596 Ferreira, M., Kajin, M., Vieira, M., Zangrandi, P., Cerqueira, R. & Gentile, R. (2013). Life
597   history of a neotropical marsupial: Evaluating potential contributions of survival and
598   reproduction to population growth rate. *Mamm Biol*, 78, 406–411.

599 Franco, M. & Silvertown, J. (2004). A comparative demography of plants based upon
600   elasticities of vital rates. *Ecology*, 85, 531–538.

Gaillard, J.-M. & Yoccoz, N. (2003). Temporal Variation in Survival of Mammals: a Case of Environmental Canalization? *Ecology*, 84, 3294–3306.

Gillespie, J.H. (1977). Natural Selection for Variances in Offspring Numbers: A New Evolutionary Principle. *Am Nat*, 111, 1010–1014.

Griffith, A.B. (2017). Perturbation approaches for integral projection models. *Oikos*, 126, 1675–1686.

Haridas, C.V. & Tuljapurkar, S. (2005). Elasticities in Variable Environments: Properties and Implications. *Am Nat*, 166, 481–495.

Healy, K., Ezard, T.H.G., Jones, O.R., Salguero-Gómez, R. & Buckley, Y.M. (2019). Animal life history is shaped by the pace of life and the distribution of age-specific mortality and reproduction. *Nat Ecol Evol*, 3, 1217–1224.

Heppell, S.S. (1998). Application of Life-History Theory and Population Model Analysis to Turtle Conservation. *Copeia*, 1998, 367.

Hilde, C.H., Gamelon, M., Sæther, B.-E., Gaillard, J.-M., Yoccoz, N.G. & Pélabon, C. (2020). The Demographic Buffering Hypothesis: Evidence and Challenges. *Trends Ecol Evol*, 35, 523–538.

Jäkäläniemi, A., Ramula, S. & Tuomi, J. (2013). Variability of important vital rates challenges the demographic buffering hypothesis. *Evol Ecol*, 27, 533–545.

Jones, J.H. (2007). demogR: A Package for the Construction and Analysis of Age-structured Demographic Models in R. *J Stat Softw*, 22, 1–28.

Jones, J.H. (2011). Primates and the evolution of long, slow life histories. *Current Biology*, 21, R708–R717.

Jongejans, E., De Kroon, H., Tuljapurkar, S. & Shea, K. (2010). Plant populations track rather than buffer climate fluctuations. *Ecol Lett*, 13, 736–743.

Koons, D.N., Pavard, S., Baudisch, A. & Jessica E. Metcalf, C. (2009). Is life-history buffering or lability adaptive in stochastic environments? *Oikos*, 118, 972–980.

Kroon, H. de, van Groenendael, J. & Ehrlen, J. (2000). Elasticities: A review of methods and model limitations.

McDonald, J.L., Franco, M., Townley, S., Ezard, T.H.G., Jelbert, K. & Hodgson, D.J. (2017). Divergent demographic strategies of plants in variable environments. *Nat Ecol Evol*, 1, 0029.

Morris, W.F., Altmann, J., Brockman, D.K., Cords, M., Fedigan, L.M., Pusey, A.E., *et al.* (2011). Low Demographic Variability in Wild Primate Populations: Fitness Impacts of Variation, Covariation, and Serial Correlation in Vital Rates. *Am Nat*, 177, E14–E28.

Morris, W.F. & Doak, D.F. (2004). Buffering of Life Histories against Environmental Stochasticity: Accounting for a Spurious Correlation between the Variabilities of Vital Rates and Their Contributions to Fitness. *Am Nat*, 163, 579–590.

638   Morris, W.F., Pfister, C.A., Tuljapurkar, S., Haridas, C. V., Boggs, C.L., Boyce, M.S., *et al.*
639   (2008). Longevity can buffer plant and animal populations against changing climatic
640   variability. *Ecology*, 89, 19–25.

641   Pélabon, C., Hilde, C.H., Einum, S. & Gamelon, M. (2020). On the use of the coefficient of
642   variation to quantify and compare trait variation. *Evol Lett*, 4, 180–188.

643   Pfister, C. (1998). Patterns of variance in stage-structured populations: Evolutionary
644   predictions and ecological implications. *Proceedings of the National Academy of*
645   *Sciences*, 95, 213–218.

646   Reed, A.W. & Slade, N.A. (2012). Buffering and plasticity in vital rates of oldfield rodents.
647   *Journal of Animal Ecology*, 81, 953–959.

648   Rodríguez-Caro, R.C., Capdevila, P., Graciá, E., Barbosa, J.M., Giménez, A. & Salguero-
649   Gómez, R. (2020). The demographic buffering strategy has a threshold of effectiveness
650   to increases in environmental stochasticity. *bioRxiv*, 1–41.

651   Roff, D.A. & Fairbairn, D.J. (2007). The evolution of trade-offs: Where are we? *J Evol Biol*,
652   20, 433–447.

653   Rotella, J.J., Link, W.A., Chambert, T., Stauffer, G.E. & Garrott, R.A. (2012). Evaluating the
654   demographic buffering hypothesis with vital rates estimated for Weddell seals from 30
655   years of mark – recapture data, 162–173.

656   Salguero-Gómez, R., Jones, O.R., Archer, C.R., Bein, C., de Buhr, H., Farack, C., *et al.*
657   (2016). COMADRE: A global data base of animal demography. *Journal of Animal*
658   *Ecology*, 85, 371–384.

659   Shyu, E. & Caswell, H. (2014). Calculating second derivatives of population growth rates for
660   ecology and evolution. *Methods Ecol Evol*, 5, 473–482.

661   Stearns, S. (1992). *The Evolution of Life Histories*. Oxford University Press, New York,
662   USA.

663   Stearns, S.C. (1983). The Influence of Size and Phylogeny on Patterns of Covariation among
664   Life-History Traits in the Mammals. *Oikos*, 41, 173.

665   Sutherland, W.J., Freckleton, R.P., Godfray, H.C.J., Beissinger, S.R., Benton, T., Cameron,
666   D.D., *et al.* (2013). Identification of 100 fundamental ecological questions. *Journal of*
667   *Ecology*, 101, 58–67.

668   Tuljapurkar, S., Gaillard, J.-M. & Coulson, T. (2009). From stochastic environments to life
669   histories and back. *Philosophical Transactions of the Royal Society B: Biological*
670   *Sciences*, 364, 1499–1509.

671   Tuljapurkar, S., Horvitz, C.C. & Pascarella, J.B. (2003). The Many Growth Rates and
672   Elasticities of Populations in Random Environments. *Am Nat*, 162, 489–502.

673   Tuljapurkar, S.D. (1982). Population dynamics in variable environments. III. Evolutionary
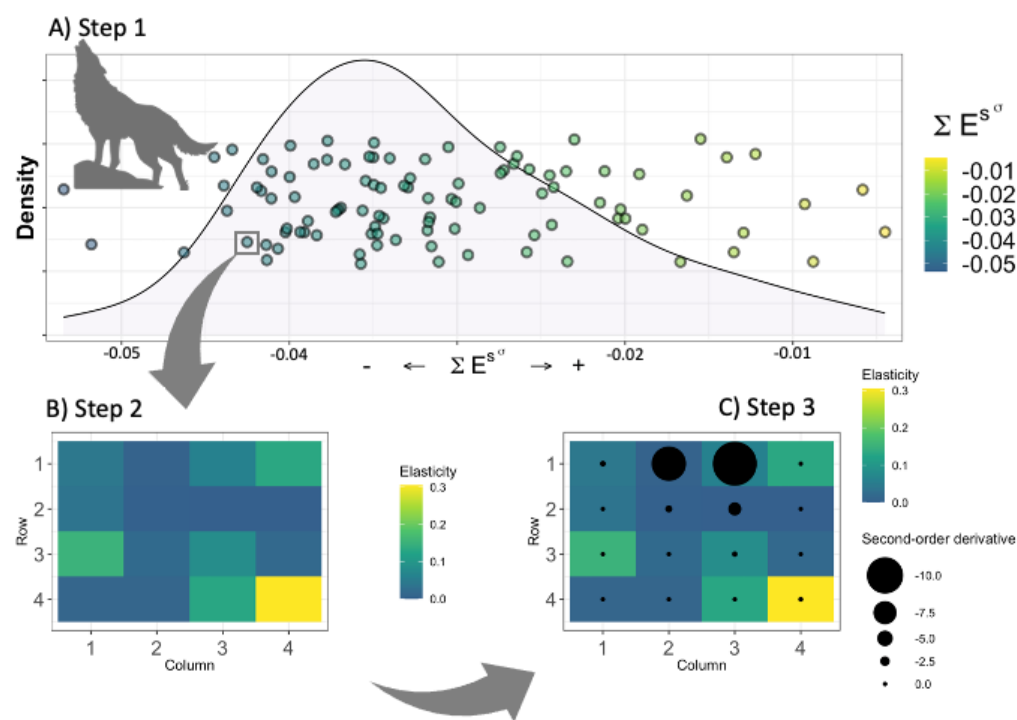674   dynamics of r-selection. *Theor Popul Biol*, 21, 141–165.

675 Tuljapurkar, S. (1990). Population Dynamics in Variable Environments. In: *Lecture notes in*
676   *Biomathematics*, Lecture Notes in Biomathematics (ed. Levin, S.). Springer Berlin
677   Heidelberg.

678 Vázquez, D.P., Gianoli, E., Morris, W.F. & Bozinovic, F. (2017). Ecological and
679   evolutionary impacts of changing climatic variability. *Biological Reviews*, 92, 22–42.
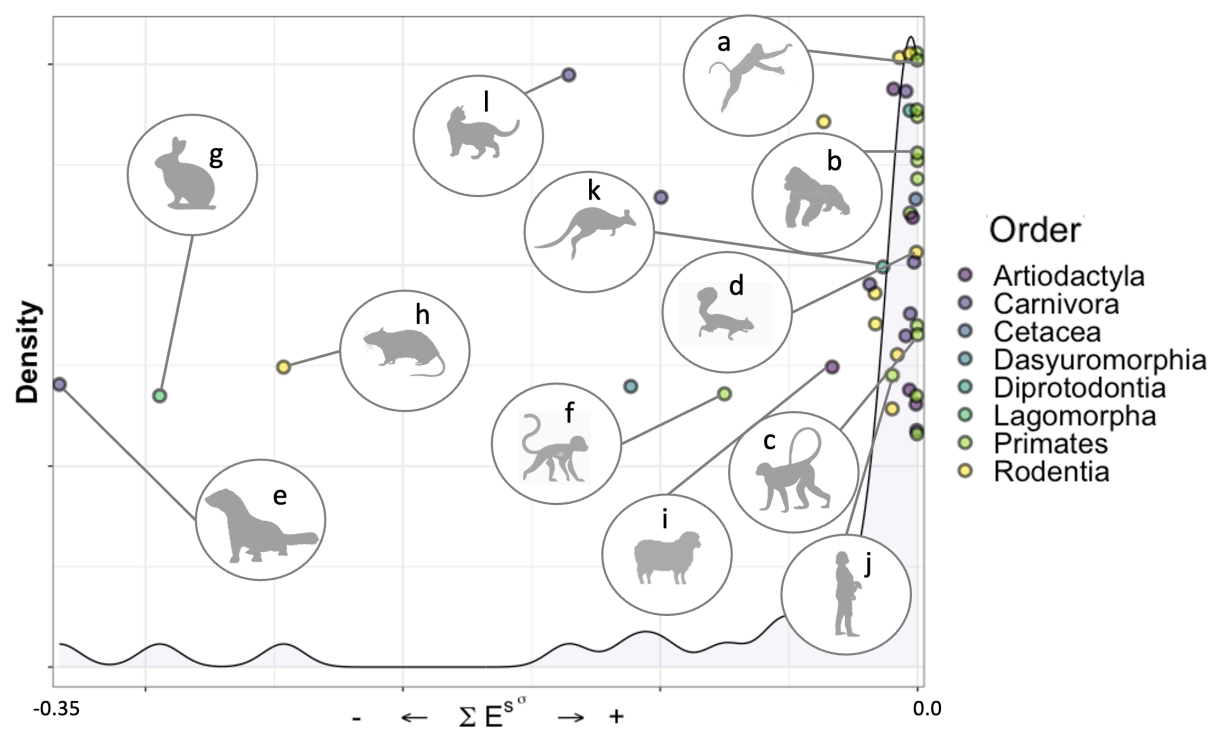
680 Wang, J., Yang, X., Silva Santos, G., Ning, H., Li, T., Zhao, W., *et al.* (2023). Flexible
681   demographic strategies promote the population persistence of a pioneer conifer tree
682   (Pinus massoniana) in ecological restoration. *For Ecol Manage*, 529, 120727.

683

684

Figure 1
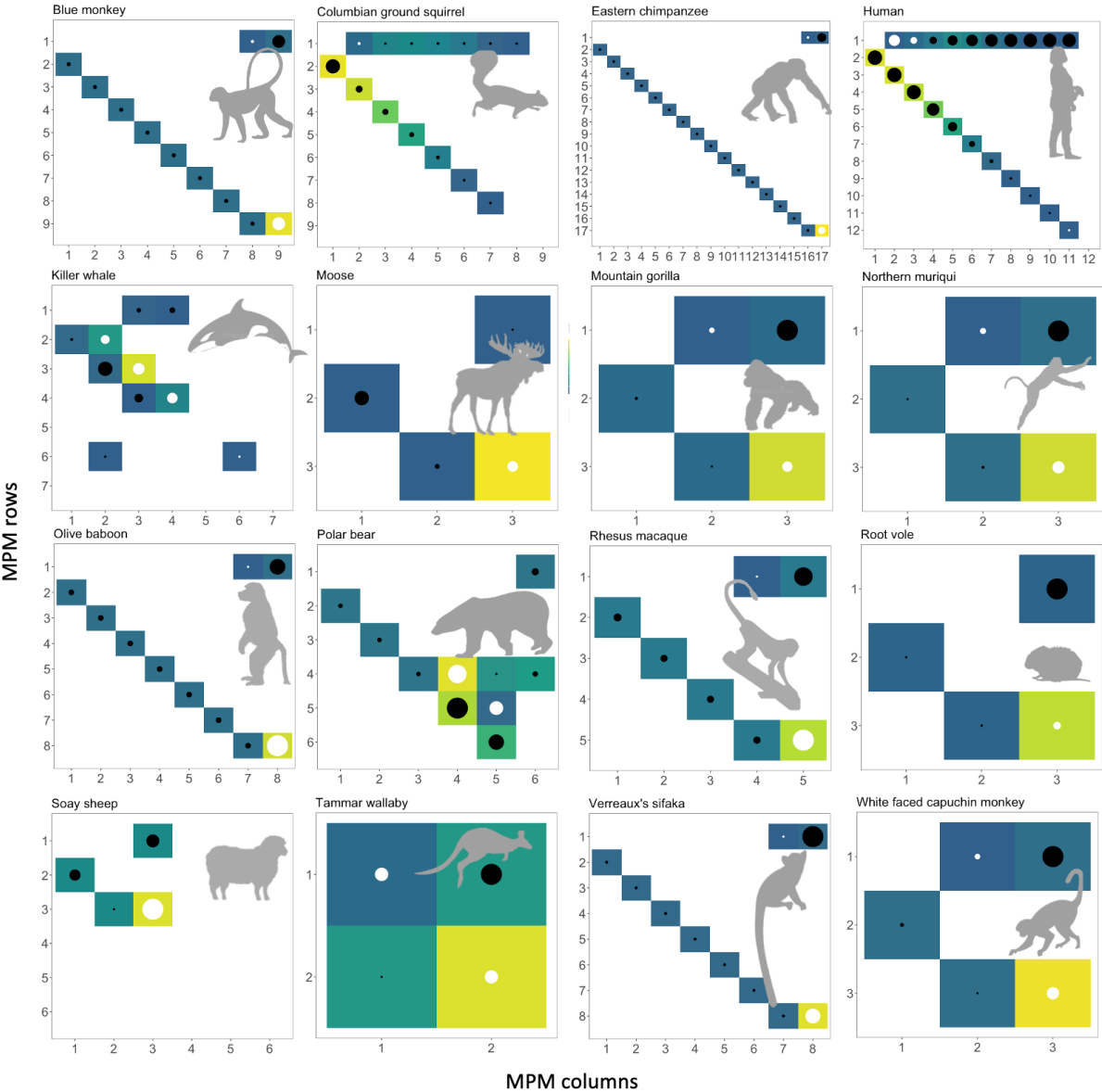
Figure 2

Figure 3

Figure legends

695

696   **Figure 1**. A three-step framework proposed to: Step 1 - allocate species and/or populations

697   on a variance continuum (plot A, dots representing 50 hypothetical species). The variance

698   continuum operates at the between-populations level (see text) and is represented by

699   partitioning the sum of all the stochastic elasticities ($\Sigma E_{a_{ij}}^{S}$) into two compounds: i) sums of

700   stochastic elasticities with respect to the variance ($\Sigma E_{a_{ij}}^{S^{\sigma}}$), and ii) sums of stochastic

701   elasticities with respect to the mean ($\Sigma E_{a_{ij}}^{S^{\mu}}$). The first step of our framework shows the

702   variance compound of the sums of stochastic elasticities forming a continuum where the

703   right-hand side of the plot represents species (or populations) where a perturbation of

704   variance in demographic processes results in weak or no impact on λ_s (yellow dots). The

705   yellow-dotted species (or populations) can be classified as having potentially *buffered life-*

706   *cycles* – based on all the demographic processes. The left-hand side of the graph represents

707   species (or populations) where a perturbation of the variance in demographic processes

708   results in strong impact on λ_s (blue dots). Thus, the blue-dotted species (or populations) can

709   be classified as having potentially *unbuffered life cycles* – based on all the demographic

710   processes. The vertical axis delineates the values of the density distribution function,

711   indicating the number of species/populations at each value of $\Sigma E_{a_{ij}}^{S^{\sigma}}$. The placement of data

712   points (species/populations) along the horizontal axis corresponds to their calculated values

713   of $\Sigma E_{a_{ij}}^{S^{\sigma}}$ and is arranged linearly, while the breadth along the y-axis is solely for improved

714   visual comprehension. Step 2 - Access the linear selection pressures for individual species or

715   populations at within-species level (see text) (plot B). Step 2 displays the elasticities of the

716   deterministic population growth rate (λ_t) for a hypothetical population of wolf and reveals the

717   linear selection gradients, and which demographic processes are the most influential for λ_t.

718   Step 3 - Access the nonlinear selection pressures at the within-species level (see text) (plot

C). In the third step self-second derivatives for the corresponding demographic processes

from step 2 are displayed.

Figure 2. Results for step 1 of our framework showing the sum of stochastic elasticities with respect to the variance $\Sigma E_{a_{ij}}^{S^\sigma}$. The closer the $\Sigma E_{a_{ij}}^{S^\sigma}$ is to zero, the weaker the impact of variation in demographic processes on λ_s. The 40 populations from 34 species of mammals from the COMADRE database are ranked into the variance continuum from potentially buffered (right-hand side) to less buffered (left-hand side), since any variation in demographic processes would strongly impact λ_s. Colors represent different taxonomic orders with Primates occupying the right-hand side. Silhouettes: a) *Brachyteles hyphoxantus*, b) *Gorilla beringhei*, c) *Cercopithecus mitis*, d) *Urocitellus columbianus,* e) *Mustela erminea*, f) *Erythrocebus patas*, g) *Lepus americanus*, h) *Rattus fuscipes*, i) *Ovis aries*, j) *Homo sapiens*, k) *Macropus eugenii*, and l) *Felis catus*. The vertical axis delineates the values of the density distribution function, indicating the number of species/populations at each value of $\Sigma E_{a_{ij}}^{S^\sigma}$. The placement of data points (species/populations) along the horizontal axis corresponds to their calculated values of $\Sigma E_{a_{ij}}^{S^\sigma}$ and is arranged linearly, while the breadth along the y-axis is solely for improved visual comprehension.

Figure 3: Results from steps 2 and 3 of the proposed framework (see Fig. 2B, C). The 16 plots represent populations where the MPMs built by ages were available in the COMADRE database (see text). The color scale represents elasticity values for each of the demographic processes in the MPM, where yellow represents high and blue low elasticity values. No color means elasticity=0. Because the aim of step 2 is to identify the most impacting demographic process within each species' life cycle (the within-populations level, see text) - not to

743 compare the elasticity values among species - each plot has its own scale (see end of legend).

744 The black dots represent negative self-second derivatives of λ_t - thus concave selection - and

745 the white dots represent positive self-second derivatives of λ_t - thus convex selection. The dot

746 sizes are scaled by the absolute value of self-second derivatives, where the smaller the dot,

747 the closer a self-second derivative is to 0, indicting weak or no nonlinearity. Large dots

748 indicate strong nonlinear selection forces. Scales ($E_{min-max}$=elasticity minimum and maximum

749 value, $SSD_{min-max}$=self-second derivative minimum and maximum value): Blue monkey $E_{min-max}$=0.00-0.52, $SSD_{min-max}$=-1.25-1.27; Columbian ground squirrel: $E_{min-max}$=0.00-0.23,

750 $SSD_{min-max}$=-1.48-0.01; Eastern chimpanzee: $E_{min-max}$=0.00-0.60, $SSD_{min-max}$=-4.39-2.59;

751

752 Human: $E_{min-max}$=0.00-0.18, $SSD_{min-max}$=-0.15-0.08; Killer whale: $E_{min-max}$=0.00-0.55,

753 $SSD_{min-max}$=-5.72-3.43; Moose: $E_{min-max}$=0.00-0.55, $SSD_{min-max}$=-0.66-0.36; Mountain gorilla:

754 $E_{min-max}$=0.00-0.81, $SSD_{min-max}$=-1.46-0.28; Northern muriqui: $E_{min-max}$=0.00-0.72, $SSD_{min-max}$=-1.17-0.35; Olive baboon: $E_{min-max}$=0.00-0.54, $SSD_{min-max}$=-0.57-1.13; Polar bear: $E_{min-max}$=0.00-0.26, $SSD_{min-max}$=-0.73-0.54; Rhesus macaque: $E_{min-max}$=0.00-0.51, $SSD_{min-max}$=-0.54-0.71; Root vole: $E_{min-max}$=0.00-0.86, $SSD_{min-max}$=-2.54-0.22; Soay sheep: $E_{min-max}$=0.00-0.56, $SSD_{min-max}$=-0.22-0.40; Tammar wallaby: $E_{min-max}$=0.00-0.55, $SSD_{min-max}$=-0.64-0.34;

755

756

757

758

759 White faced capuchin monkey: $E_{min-max}$=0.00-0.66, $SSD_{min-max}$=-2.66-1.21.

760

Supplementary material – Data available in COMADRE Version 2.0.1 and results from Step 1 of the framework

762 **Table S1.** The metadata used in step 1 of our framework and the respective results presented in the main text. The first four columns represent

763 the information from where Matrix Populations Models (MPMs) were extract precisely as presented in COMADRE 2.0.1. Column titles differ

764 from the database as "SpeciesAuthorComadre" is equivalent to "SpeciesAuthor" and "SpeciesName" is equivalent to "SpeciesAccepted" in

765 COMADRE 2.0.1. The remaining columns present the results of step 1, where we present the raw values of $\Sigma E_{a_{ij}}^{S^{\mu}}$ and $\Sigma E_{a_{ij}}^{S^{\sigma}}$, their respective

766 standard deviation, the stochastic population growth rate λ_s, and the number of available matrices (# matrices). For ByAge, "TRUE" was

767 assigned for MPMs built by age or "FALSE" if otherwise.

SpeciesAuthorComadre	SpeciesName	CommonName	Order	$\Sigma E_{a_{ij}}^{S^{\mu}}$	$\Sigma E_{a_{ij}}^{S^{\mu}}$ (sd)	$\Sigma E_{a_{ij}}^{S^{\sigma}}$	$\Sigma E_{a_{ij}}^{S^{\sigma}}$ (sd)	# matrices	λ
Homo_sapiens_subsp._sapiens	*Homo sapiens sapiens*	Human	Primates	1.003	0.003	1.003	0.004	13	1.064
Alces_alces	*Alces alces*	Moose	Artiodactyla	1.001	0.001	1.001	0.001	13	1.205
Antechinus_agilis	*Antechinus agilis*	Agile antechinus	Dasyuromorphia	1.111	0.111	1.111	0.011	2	0.931
Brachyteles_hypoxanthus	*Brachyteles hypoxanthus*	Northern muriqui	Primates	1.000	0.000	1.000	0.000	12	1.051
Callospermophilus_lateralis	*Callospermophilus lateralis*	Golden-mantled ground squirrel	Rodentia	1.054	0.054	1.054	0.055	9	2.052
Cebus_capucinus	*Cebus capucinus*	White faced capuchin monkey	Primates	1.000	0.000	1.000	0.000	11	1.021
Cercopithecus_mitis	*Cercopithecus mitis*	Blue monkey	Primates	1.000	0.000	1.000	0.000	14	1.036
Eumetopias_jubatus	*Eumetopias jubatus*	Northern sea lion; Steller sea lion	Carnivora	1.005	0.005	1.005	0.002	2	0.904
Felis_catus	*Felis catus*	Feral cat	Carnivora	1.136	0.136	1.136	0.012	1	1.948
Gorilla_beringei	*Gorilla beringei*	Mountain gorilla	Primates	1.000	0.000	1.000	0.000	21	1.027

Hippocamelus_bisulcus	*Hippocamelus bisulcus*	Huemul deer	Artiodactyla	1.002	0.002	1.002	0.001	1	0.996
Lepus_americanus	*Lepus americanus*	Snowshoe hare	Lagomorpha	1.294	0.294	1.294	0.165	2	0.812
Lycaon_pictus	*Lycaon pictus*	African wild dog	Carnivora	1.100	0.100	1.100	0.008	1	1.500
Macaca_mulatta_3	*Macaca mulatta*	Rhesus macaque	Primates	1.000	0.000	1.000	0.001	12	1.127
Macropus_eugenii	*Macropus eugenii*	Tammar wallaby	Diprotodontia	1.013	0.013	1.013	0.012	7	0.981
Marmota_flaviventris_2	*Marmota flaviventris*	Yellow-bellied marmot	Rodentia	1.007	0.007	1.007	0.006	4	0.890
Marmota_flaviventris_3	*Marmota flaviventris*	Yellow-bellied marmot	Rodentia	1.008	0.008	1.008	0.005	4	0.921
Microtus_oeconomus	*Microtus oeconomus*	Root vole	Rodentia	1.000	0.000	1.000	0.001	14	1.028
Mustela_erminea	*Mustela erminea*	Stoat	Carnivora	1.334	0.334	1.334	0.117	2	1.258
Orcinus_orca_2	*Orcinus orca*	Killer whale	Cetacea	1.001	0.001	1.001	0.001	24	0.999
Ovis_aries_2	*Ovis aries*	Soay sheep	Artiodactyla	1.033	0.033	1.033	0.020	3	1.099
Pan_troglodytes_subsp._schweinfurthii	*Pan troglodytes*	Eastern chimpanzee	Primates	1.000	0.000	1.000	0.001	22	0.982
Papio_cynocephalus	*Papio cynocephalus*	Olive baboon	Primates	1.000	0.000	1.000	0.000	19	1.054
Peromyscus_maniculatus_2	*Peromyscus maniculatus*	Deer mouse	Rodentia	1.010	0.010	1.010	0.005	2	1.107
Phocarctos_hookeri	*Phocarctos hookeri*	New Zealand sea lion	Carnivora	1.005	0.005	1.005	0.003	8	1.023
Propithecus_verreauxi	*Propithecus verreauxi*	Verreaux's sifaka	Primates	1.000	0.000	1.000	0.000	12	0.986
Puma_concolor_8	*Puma concolor*	Cougar	Carnivora	NA	NA	NA	NA	10	1.115
Rattus_fuscipes	*Rattus fuscipes*	Bush rat	Rodentia	1.246	0.246	1.246	0.029	2	1.305
Spermophilus_armatus	*Urocitellus armatus*	Uinta ground squirrel	Rodentia	1.016	0.016	1.016	0.011	4	1.125
Spermophilus_armatus_2	*Urocitellus armatus*	Uinta ground squirrel	Rodentia	1.017	0.017	1.017	0.010	3	1.095

Spermophilus_columbianus	*Urocitellus columbianus*	Columbian ground squirrel	Rodentia	1.036	0.036	1.036	0.025	3	1.009
Spermophilus_columbianus_3	*Urocitellus columbianus*	Columbian ground squirrel	Rodentia	1.003	0.003	1.003	0.006	3	1.200
Ursus_americanus_subsp._floridanus	*Ursus americanus*	Florida black bear	Carnivora	1.003	0.003	1.003	0.003	2	1.020
Ursus_arctos_subsp._horribilis_5	*Ursus arctos*	Grizzly bear	Carnivora	1.001	0.001	1.001	0.001	4	1.026
Ursus_maritimus_2	*Ursus maritimus*	Polar bear	Carnivora	1.019	0.019	1.019	0.007	2	0.941
Brachyteles_hypoxanthus_2	*Brachyteles hypoxanthus*	Northern muriqui	Primates	1.000	0.000	1.000	0.000	12	1.111
Cebus_capucinus_2	*Cebus capucinus*	WhiteNAfaced capuchin monkey	Primates	1.000	0.000	1.000	0.000	11	1.059
Chlorocebus_aethiops_2	*Chlorocebus aethiops*	Vervet	Primates	1.075	0.075	1.075	0.087	5	1.187
Erythrocebus_patas	*Erythrocebus patas*	Patas monkey	Primates	1.051	0.051	1.051	0.038	5	1.128
Gorilla_beringei_subsp._beringei	*Gorilla beringei*	Mountain gorilla	Primates	1.000	0.000	1.000	0.000	21	1.053

768

769